Tectonophysics, 152 (1988) 319–334
Elsevier Science Publishers B.V., Amsterdam – Printed in The Netherlands

Determination of space–time structure of a deep earthquake source by means of power moments

A.A. GUSEV and V.M. PAVLOV

Institute of Volcanology, Petropavlovsk-Kamchatsky, 683006 (U.S.S.R.)

(Received October 1, 1986; accepted January 19, 1987)

Abstract

Gusev, A.A. and Pavlov, V.M., 1988. Determination of space–time structure of a deep earthquake source by means of power moments. In: O. Kulhánek (Editor), Seismic Source Physics and Earthquake Prediction Research. *Tectonophysics*, 152: 319–334.

For a planar shear earthquake source with monotonous slip at a given point, power moments of the slip rate function provide a useful means of reconstructing a space–time source structure. In theory, even a smoothed source function can be uniformly estimated. Power moments are linear functions of the processed data.

We have developed a practical technique for estimating the source power moment of degrees 1 and 2 from the body wave pulses of deep earthquakes. The technique is applied to a moderate ($m_b = 5.7$) event in the Fiji Islands. We determined the source plane, elongation direction, length and duration values, degree of asymmetry and possible rupture velocity. Most estimates are independent from any particular parametric source model, although the Haskell-Aki partly bilateral model agrees well with our observations.

Introduction

In order to determine the space–time structure of earthquake sources, different approaches have been tried. The two most consistently applied are: (1) determination of the parameters of some source model of an a priori fixed functional form, and (2) representation of the source as the superposition of a number of simple subsources (point sources or dislocations) by trial and error. Both approaches have demonstrated their usefulness. They both have, however, one important disadvantage: the functional form of the source or subsource is fixed arbitrarily. Therefore, it would be useful to consider another kind of approach, which would be more or less free from a priori assumptions. The approach presented here is of this kind; it is based on specifying the source according to its power moments.

This kind of approach was first proposed by Goltzman (1971), who suggested that an imaginary elastic wave radiator be represented in seismic prospecting by its set of power moments. Backus and Mulkahy (1976a,b) used power moments to describe a general seismic source. They mentioned that power moments can be used to determine the low-frequency component of a radiation field, but they did not consider inversion. The present authors (Gusev and Pavlov, 1978; Pavlov and Gusev, 1980) derived equations connecting space–time source power moments and time power moments of body wave pulses. For a planar shear source with a positive slip rate function these equations allow us to determine, in theory, all source power moments up to a certain degree K, K depending on the quantity and accuracy of the data available. It was also shown that with the set of power moments up to degree K at hand, one

0040-1951/88/$03.50

can determine the smoothed version of the slip rate function, thus completing, in a sense, the inversion of a planar shear source. These results are described in detail in Gusev and Pavlov (1982).

Based on the approach of Backus and Mulkahy, Doornbos (1982a,b) determined source moments of degrees 1 and 2 for a deep earthquake. Silver (1983) derived equations for degree 2 moments, and in Silver and Matsuda (1985) these moments were determined for two surface focus earthquakes.

The present paper includes a summary of our theoretical studies (Gusev and Pavlov, 1978, 1982; Pavlov and Gusev, 1980) and an example of their application (presented in greater detail in Pavlov and Gusev (1986) and in Gusev and Pavlov (1986a,b).

Three-dimensional source power moments and their relation to body wave field

We shall consider the earthquake source model of planar shear rupture. As the rupture plane is not known beforehand, we shall also consider a somewhat more general volume source model. Both models are essentially scalar ones: volume or surface seismic moment density at a point is defined by the product of a constant tensor with the scalar function of point and time. This model is much less general than that of Backus and Mulkahy (1976a,b), and it is clear that for some earthquakes it will not be correct. We hope, however, that in many cases the main part of the source motion of a real earthquake can be idealized by plane shear rupture. It should be mentioned that the approach presented here is applicable to any planar source that can be decomposed as described above, e.g., tensile crack or a dense planar set of dilatation sources.

So let us introduce two source models, A and B. For model A, the source is located in the limited volume V of a homogeneous elastic medium, and is described by the volume density of the seismic moment:

$$m_{ij}(t,\boldsymbol{x}) = m_{ij}^{(0)} f^{v}(t,\ \boldsymbol{x})$$

where $i,\ j = 1,\ 2,\ 3$. $\boldsymbol{x} = \{x_1,\ x_2,\ x_3\}$ are the Cartesian coordinates, t is time, and $m_{ij}^{(0)} = m_{ji}^{(0)}$ is the constant "unit" tensor: $\frac{1}{2} m_{ij}^{(0)} m_{ij}^{(0)} = 1$; the summation convention is assumed here and below. For model B, the source is a shear rupture in a limited area S of a plane Σ with unit normal $\boldsymbol{n}$, with displacement jump (slip) function $\boldsymbol{B}(t,\ \boldsymbol{x}) = \boldsymbol{b} f^{\Sigma}(t,\ \boldsymbol{x})$. The direction of slip $\boldsymbol{B}$ is constant, $\boldsymbol{b} \cdot \boldsymbol{n} = 0$, and $|\boldsymbol{b}| = 1$. Model B is a particular case of model A when:

$$m_{ij}^{(0)} = n_i b_j + n_j b_i$$

$$f^{v}(t,\ \boldsymbol{x}) = \mu f^{\Sigma}(t,\ \boldsymbol{x}) \delta_{\Sigma}(\boldsymbol{x}) \tag{1}$$

where $\delta_{\Sigma}(\boldsymbol{x})$ is a surface Dirac delta function on Σ and μ is the shear modulus.

We assume that the source process starts at a fixed point, the hypocentre, and at a fixed moment in time, and we choose the origin of the coordinate system at the hypocentre, and let $t = 0$ for the moment when rupture begins. The process does not leave V (or S) and finishes at the moment $t = T$. We shall also introduce an important assumption concerning the monotonous increase of plastic deformation or slip at a given point. This assumption is plausible from a physical point of view. We assume that it can be disturbed only on a local scale and that this disturbance is negligible. Formally our assumptions can be written as follows ($\dot{\phi} \equiv \partial\phi/\partial t$):

$$\left.\begin{array}{lll} (1) & f^{v} = 0 & \text{and } f^{\Sigma} = 0 \text{ at } t < 0 \\ (2) & \dot{f}^{v} = 0 & \text{and } \dot{f}^{\Sigma} = 0 \text{ at } t > T \\ (3) & \dot{f}^{v} \geqslant 0 & \text{and } \dot{f}^{\Sigma} \geqslant 0 \text{ at } 0 < t < T \\ (4) & f^{v} = 0 & \text{outside } V,\ f^{\Sigma} = 0 \\ & & \text{outside } S \end{array}\right| \tag{2}$$

To introduce (normalized) power moments for the source we use the function:

$$L(\phi) = \int_V \int_0^T \phi(t,\ \boldsymbol{x}) \dot{f}^{v}(t,\ \boldsymbol{x})\ \mathrm{d}t\ \mathrm{d}V$$

Initial moments of degree 1 are defined as:

$$N_\alpha = L(x_\alpha)/L(1) \qquad (\alpha = 0,\ 1,\ 2,\ 3,\ x_0 \equiv t) \tag{3}$$

initial and central moments of degree 2 as:

$$\left.\begin{array}{l} N_{\alpha\beta}^{(0)} = L(x_\alpha x_\beta)/L(1) \\ N_{\alpha\beta} = N_{\alpha\beta}^{(0)} - N_\alpha N_\beta \end{array}\right\}$$

$$(\alpha,\ \beta = 0,\ 1,\ 2,\ 3,\ x_0 \equiv t) \tag{4}$$

For planar source, the functional L takes the form:

$$L(\phi) = \int_{\Sigma}\int_{0}^{T} \phi(t, \boldsymbol{x}) f^{\Sigma}(t, \boldsymbol{x})\, \mathrm{d}t\, \mathrm{d}S$$

In this case, some specific relations are true for power moments, namely:

$$\left.\begin{aligned} n_i N_i &= 0 \\ n_i N_{i0} &= 0 \\ n_i N_{ij} &= 0 \end{aligned}\right\} \qquad (i, j = 1, 2, 3) \tag{5}$$

The value $L(1)$ is identical to the usual scalar seismic moment M_0. It is convenient to introduce notations: $N_t \equiv N_0$, $N_{tt} \equiv N_{00}$, $N_{it} \equiv N_{i0}$ $(i = 1, 2, 3)$. The dimensions of the power moments are: N_t [s], N_i [km], N_{tt} [s^2], N_{it} (km · s], N_{ij} [km^2]; from these dimensions one can see the sort of moment (space, time or space–time). Values N_t and N_{tt} are scalars; the sets $\{N_1, N_2, N_3\}$ and $\{N_{1t}, N_{2t}, N_{3t}\}$ are vectors, and will be referred to as $\boldsymbol{d}$ and $\boldsymbol{q}$ respectively. The matrix N_{ij} $(i, j = 1, 2, 3)$ represents a symmetrical tensor.

Let $u(t, \boldsymbol{r})$ be a far-field body wave (e.g., a P-wave) displacement, produced by our source and radiated along the ray $\boldsymbol{r}$ $(|\boldsymbol{r}| = 1)$. According to our assumptions, the pulse shape of u is unipolar, with a definite beginning and end. Now let us introduce power moments of u. For degrees 1 and 2 we have:

$$\left.\begin{aligned} e_1^{(0)}(\boldsymbol{r}) &\equiv e_1(\boldsymbol{r}) \\ &= \frac{1}{E_0}\int_{t_1}^{t_2} u(t, \boldsymbol{r})(t - t_1)\, \mathrm{d}t \\ e_2^{(0)}(\boldsymbol{r}) &= \frac{1}{E_0}\int_{t_1}^{t_2} u(t, \boldsymbol{r})(t - t_1)^2\, \mathrm{d}t \\ e_2 &= e_2^{(0)} - e_1^2 \end{aligned}\right| \tag{6}$$

where $E_0 \equiv E_0(\boldsymbol{r}) = \int_{t_1}^{t_2} u(t, \boldsymbol{r})\mathrm{d}t$ is the pulse "area", t_1 is the onset time and t_2 is the end moment of the pulse. It is clear that instead of u, one can use the projection of vector displacement onto any axis.

To connect pulse and source power moments, let us write the far-field vector displacement u_i for an infinite homogeneous medium. For source model A:

$$u_i(t, \boldsymbol{r}) = Q_i \int_V \dot{f}^v(t - R/c + \boldsymbol{x}\cdot\boldsymbol{r}/c, \boldsymbol{x})\, \mathrm{d}V \tag{7}$$

where $c = c_\mathrm{p}$ or c_s is the wave velocity, R is the distance to the observation point, and Q_i is a factor which for a P-wave, for example, is equal to:

$$Q_i = r_i r_j r_k m_{jk}^{(0)} / 4\pi\rho c_\mathrm{p}^3 R$$

where ρ is the density. For both P- and S-waves, Q_i (which includes both geometrical spreading and the radiation pattern) will cancel afterwards. For subsonic rupture, R/c coincides with the onset time t_1, and this case will be presumed below. Let us multiply both sides of (7) by $(t - R/c)^K$ $(K = 0, 1, 2, \ldots)$:

$$\int_{-\infty}^{\infty} u_i(t, \boldsymbol{r})(t - R/c)^K\, \mathrm{d}t$$

$$= Q_i \int_V \int_{-\infty}^{\infty} \dot{f}^v(\tau, \boldsymbol{x})(\tau - \boldsymbol{x}\cdot\boldsymbol{r}/c)^K\, \mathrm{d}\tau\, \mathrm{d}V \tag{8}$$

For $K = 0$ in particular:

$$\int_{-\infty}^{\infty} u_i(t, \boldsymbol{r})\, \mathrm{d}t = Q_i \int_V \int_{-\infty}^{\infty} \dot{f}^v(\tau, \boldsymbol{x})\, \mathrm{d}\tau\, \mathrm{d}V \tag{9}$$

Now using the binomial theorem in the right-hand side of (8) and dividing each side of (8) by each side of (9), we obtain:

$$e_K^{(0)}(\boldsymbol{r}) = \sum_{\substack{\alpha+\beta+\gamma+\delta=K \\ \alpha\geqslant 0,\ \beta\geqslant 0,\ \gamma\geqslant 0,\ \delta\geqslant 0}} A_{\alpha\beta\gamma\delta} P_{\alpha\beta\gamma\delta} \tag{10}$$

where:

$$A_{\alpha\beta\gamma\delta} = (-r_1/c)^\beta (-r_2/c)^\gamma (-r_3/c)^\delta \frac{K!}{\alpha!\beta!\gamma!\delta!}$$

are the coefficients depending on $\boldsymbol{r}$, and:

$$P_{\alpha\beta\gamma\delta} = L\left(x_0^\alpha x_1^\beta x_2^\gamma x_3^\delta\right)/L(1) \qquad (x_0 \equiv t)$$

are the power moments in general notation. In particular, for $K = 1$:

$$P_{1000} \equiv N_0 \equiv N_t, \quad P_{0100} \equiv N_1, \ldots,$$

for $K = 2$:

$$P_{2000} \equiv N_{00}^{(0)} \equiv N_{tt}^{(0)}, \quad P_{1100} \equiv N_{10}^{(0)} \equiv N_{1t}^{(0)}, \ldots,$$

$$P_{0.200} \equiv N_{11}^{(0)}, \quad P_{0110} \equiv N_{12}^{(0)}, \ldots.$$

For $K = 1$ and 2, (10) leads to:

$$N_t - r_i N_i / c = e_1(\boldsymbol{r}) \tag{11}$$

$$N_{tt} - 2r_i N_{it}/c + r_i r_j N_{ij}/c^2 = e_2(\boldsymbol{r}) \tag{12}$$

At a given K, eqn. (10) contains all source power moments of degree K. Thus a system of

such equations for different $\boldsymbol{r}$ taken in a sufficient number would seem to be an adequate basis for (linear) inversion. This is not the case, however. The relation $r_1^2 + r_2^2 + r_3^2 = 1$ makes the coefficients $A_{\alpha\beta\gamma\delta}$ in (10) linearly dependent in the general case, and in this case the above system degenerates.

For separate P or S data the solution in $P_{\alpha\beta\gamma\delta}$ includes $K(K^2-1)/6$ arbitrary constants, and is unique for $K=1$ only. For combined P and S data, it includes $(K-1)(K-2)(K-3)/6$ arbitrary constants, and is unique for $K=1, 2, 3$. Problems of this kind were to be expected, as we are trying to specify a 3-D function f^v of $\boldsymbol{x}$ whilst our information is about a 2-D function $\boldsymbol{u}$ of $\boldsymbol{r}$. When the source is assumed to be planar, non-uniqueness of this kind disappears.

It is worth mentioning that in terms of Backus and Mulkahy's arguments (1976a,b), this non-uniqueness arises because we try to calculate the equivalent force at the source from surface observations, and not because we calculate the seismic moment tensor density from the equivalent force (only the latter cause was discussed by Backus and Mulkahy).

The non-uniqueness discussed above is closely related to the problem of non-radiating sources in elastodynamics (scalar non-radiating sources are discussed in Friedlander, 1973). For example, it can be shown that a source with a seismic moment density described by the function:

$$f^v_{NR}(t, \boldsymbol{x}) = \left(\frac{1}{c_P^2}\frac{\partial^2}{\partial t^2} - \nabla^2\right) \times \left(\frac{1}{c_S^2}\frac{\partial^2}{\partial t^2} - \nabla^2\right) g(t, \boldsymbol{x})$$

where g is an arbitrary function, produces a zero displacement outside the support of g. Hence if we add the seismic moment density f^v_{NR} to any source function, its external field will not change. This obviously leads to non-uniqueness of inversion from any data outside the source (not only the far-field data). It can further be shown that the sources localized on a plane (in fact, a wide class of surface sources) cannot be non-radiating.

In order to eliminate non-uniqueness in the planar case, one can add eqns. (5) to a sufficient number of equations (11) and (12) to obtain two linear systems (for $K=1$ and 2) which do not degenerate (this procedure is in fact successful for any K). In practical inversion the source plane is unknown beforehand and should be determined simultaneously.

Planar source and its description

Let us consider now how the unknown source plane can be determined. If the tensor $m^{(0)}_{ij}$ is known and corresponds to shear rupture, we can assume that two versions of the plane are known, and the true version must be chosen. Hence it is useful to have a way to determine the plane independently of $m^{(0)}_{ij}$. In order to do so, we shall assume at first that the source is three-dimensional, and then use conditions (5) to determine Σ. Let us first consider a case where P and S data are used simultaneously. Then we can determine the second degree positively defined symmetrical tensor N_{ij} $(i, j = 1, 2, 3)$ analogous to a solid inertia tensor or to a covariance matrix. Let us find its eigenvectors and enumerate them in order of decreasing eigenvalues. We denote eigenvalues as N^*_{11}, N^*_{22}, N^*_{33} and corresponding unit eigenvectors as $\boldsymbol{l}^{(1)}$, $\boldsymbol{l}^{(2)}$, $\boldsymbol{l}^{(3)}$. For a general planar source, one of the three eigenvalues must be zero, and for a planar source with positive slip function, this zero eigenvalue will always be associated with N^*_{33}. So normal $\boldsymbol{n}$ to Σ coincides with $\boldsymbol{l}^{(3)}$. Another way to determine $\boldsymbol{n}$ is, for example, to use the vector product of vectors $\boldsymbol{d}$ and $\boldsymbol{q}$ (see eqn. 5) which both lie in Σ.

When only P or only S data are known, an arbitrary parameter is included in the values of 3-D source moments of degree 2. The following values are determined unequivocally, however:

$$N_{it},\ \tilde{N}_{ij} = N_{ij} + c^2 N_{tt}\delta_{ij}$$

where δ_{ij} is the Kronecker delta.

For tensors N_{ij} and $\tilde{N}_{ij}$, the eigenvectors are identical, and the decreasing order of eigenvalues is the same; so, in this case, vector $\boldsymbol{l}^{(3)}$, coinciding with vector $\boldsymbol{n}$, can also be determined. It can be stated that $N_{tt} = c^{-2}\tilde{N}_{33}$, so the use of conditions (5) enables us to avoid arbitrariness in the values of 3-D moments of degree 2.

When the plane Σ is found, it is convenient to rotate the initial coordinate system to coincide axis x_3 with $\boldsymbol{n}$. N_3 and all $N_{\alpha\beta}$ with $\alpha = 3$ or $\beta = 3$ must now be equal to zero, and this condition can be set in advance. Now the number of unknowns reduces to 3 for degree 1 and to 6 for degree 2. Power moments in this case will be referred to as two-dimensional, and will be denoted by a bar above them. They can be determined by the least-squares technique from somewhat modified versions of eqns. (11) or (12). Modification includes changing the coordinate system and exclusion of all unknowns that must be equal to zero. For 2-D moments, the (overdetermined) least-squares system does not degenerate for any K. Formally, the last step is excessive when we consider ideal data, but it is very useful in real cases, and is even formally necessary for the determination of high degree moments.

The set of source 2-D power moments of degrees 1 and 2 is the main formal result of the approach presented here, but for physical interpretation some functions of these moments are useful (see also Backus, 1977; Gusev and Pavlov, 1978, 1982). We shall list those values which specify the space–time structure of the source in our approach. The linear dimensions of a "static" source (defined by the function $f^{\Sigma}(\infty, \boldsymbol{x})$) are characterized by the mean square radii $R_1 = (N_{11}^*)^{0.5}$ and $R_2 = (N_{22}^*)^{0.5}$; source duration is characterized by $R_t(N_{tt})^{0.5}$. These values correspond to standard deviations in the theory of probability. The centroid of a static source (with respect to hypocentre) and the time centroid are defined by vector $\boldsymbol{d}$ and by scalar N_t, respectively. The long axis of a static source is defined by $\boldsymbol{l}^{(1)}$, and its aspect ratio by R_2/R_1. The direction of source growth is defined by vector $\boldsymbol{q}$. For an elongated source, two simple measures of asymmetry (unilaterality) can be introduced: "static" $\boldsymbol{\varkappa} = \boldsymbol{d} \cdot \boldsymbol{l}^{(1)}/R_1\sqrt{3}$ and "dynamic" $\lambda = \boldsymbol{q} \cdot \boldsymbol{l}^{(1)}/R_1 R_t$. These values are normalized so that they are equal to unity for the Haskell-Aki source–narrow rectangular dislocation with unilateral rupture, and they vanish for any centrally symmetrical source.

The source dimension estimate using the R_1 value is not always obvious, so some other estimates can be used. The value $2R_1$ gives the guaranteed lower limit of the dimension (along $\boldsymbol{l}^{(1)}$) of the area where $f^{\Sigma} \neq 0$. Value $D_\alpha R_1$ gives the upper limit of the dimension of the area where not less than $\alpha\%$ of the total "mass" (that is, seismic moment) of function f^{Σ} is localized. This estimate is an implication of the Chebyshev unequality in the theory of probability. For example, at $\alpha = 90\%$, $D_\alpha = 6.32$. Finally, a parametric model can be used. In the case of the Haskell-Aki model, the source length L_{H} is 3.46 R_1. The latter estimate seems to be the most convenient when the results of the present approach are compared with those of computations based on parametric models.

Rupture velocity cannot be estimated in principle without using a parametric model as a reference. Let us accept for this purpose the Haskell-Aki model with the partly bilateral rupture, which starts at a distance d from the centre of a rectangle and propagates with velocity v in both directions, with a step-like dislocation time function. For this model, several estimates of v can be derived, e.g., $v_1 = \sqrt{3}\,(1 + \boldsymbol{\varkappa}^2) R_1/2N_t$, $v_2 = (1 + 6\boldsymbol{\varkappa}^2 - 3\boldsymbol{\varkappa}^4)0.5R_1/2R_t$ or $v_3 = \boldsymbol{\varkappa}(3 - \boldsymbol{\varkappa}^2) R_1^2/2N_{1t}$.

Several duration estimates can also be proposed. Using N_{tt} we can suggest R_t and $\sqrt{12}\,R_t$. The last value is the accurate duration estimate for the purely unilateral or purely symmetrical Haskell-Aki source. For the model described above, another partly bilateral estimate can be suggested: $T_{\mathrm{H}} = (d + L_{\mathrm{H}}/2)/v$. As the rupture is perfectly asymmetrical along the time axis, the value $2N_t$ can also be used to estimate duration.

Accuracy estimates for moment values can be extracted by the least-squares technique. Values N_{ii}^* and $l_j^{(i)}$ depend nonlinearly on degree 2 moment values. For them, and for $|\boldsymbol{d}|$, $|\boldsymbol{q}|$ and unit vectors along $\boldsymbol{d}$ and $\boldsymbol{q}$, a special Monte-Carlo type procedure was used. For other values depending on power moments, simple "error transfer" estimates were used.

Inverse problem for a planar source

It has been shown above that for ideal observations, when the least-squares errors can be neglected, the source plane Σ and all the source power moments up to degree K (depending on the

number of observations) can be found. It is obviously interesting to look at what can be inferred from this information about function $f^{\Sigma}(t, \boldsymbol{x})$. It is known (Kostrov, 1975) that the problem of reconstruction of $f^{\Sigma}(t, \boldsymbol{x})$ from the wave far-field $u(t, r)$ is not stable. Besides, an arbitrary function cannot be approximated by any finite number of its power moments. Hence, to be solvable, the inverse problem has to be formulated in some special way.

Let us consider the positive function $\phi(t, x_1', x_2') = f^{\Sigma}(t, x_1, x_2, x_3)$ ($x_3' = 0$ is Σ) and, instead of determining ϕ, let us look at the problem of determining the smoothed (low-pass filtered) function $\phi^* = \phi * h$ (h is the smoothing kernel (window), and * denotes convolution). Let the 3-D moments in the system (t, x_1', x_2', x_3') be $P'_{\alpha\beta\gamma\delta}$ (for planar source $P'_{\alpha\beta\gamma\delta} = 0$ when $\delta \leq 0$), denote $P_{\alpha\beta\gamma} = P'_{\alpha\beta\gamma 0}$, and drop the prime from x_1', x_2'. For the Fourier transform $\tilde{\phi}(\omega, k_1, k_2)$ of $\phi(t, x_1, x_2)$ the following formal series expansion is valid:

$$\tilde{\phi}(\omega, k_1, k_2) = \frac{M_0}{\mu} \sum_{q=0}^{\infty} \sum_{\substack{\alpha+\beta+\gamma=q \\ \alpha,\beta,\gamma \geq 0}} (-i)^q \frac{P_{\alpha\beta\gamma}}{\alpha!\beta!\gamma!} \omega^{\alpha} k_1^{\beta} k_2^{\gamma} \quad (i^2 = -1) \tag{13}$$

Let us consider the series in the right-hand side truncated to the number K, and denote this truncated series as $\tilde{\phi}_K(\omega, k_1, k_2)$. Function $\phi_K(t, x_1, x_2)$ is not near to $\phi(t, x_1, x_2)$. For some h "windows", however, $\phi_K * h$ is uniformly near to $\phi * h$. Let us consider the simplest case when the window provides equal relative resolution along all three axes, t, x_1 and x_2, and when the window spectral shape $\tilde{h}(\omega, k_1, k_2)$ is 3-D "boxcar"-shaped:

$$\tilde{h}(\omega, k_1, k_2) = \Pi\left(\frac{|\omega|}{a}\right) \Pi\left(\frac{|k_1|}{b}\right) \Pi\left(\frac{|k_2|}{c}\right)$$

where:

$$\Pi(\xi) = \begin{cases} 1, & \xi \leq 1 \\ 0, & \xi > 1 \end{cases}$$

and parameters a, b and c satisfy the condition $aT = bL = cW = n$, where n is the number of resolvable elements ("pixels") along any axis, and T, L and W are characteristic dimensions, which are proportional to R_t, R_1 and R_2 (e.g., $T = \sqrt{12}\, R_t$ and so on). In this case (in Gusev and Pavlov, 1982), the simple upper limit for relative accuracy was obtained for non-negative ϕ:

$$\epsilon = \max_{t,\, x_1,\, x_2} \frac{|\phi_K^* - \phi^*|}{\bar{\phi}} < \frac{1}{\pi^3} \left[e^{3n} - \sum_{q=0}^{K+3} \frac{(3n)^q}{q!} \right] \equiv \epsilon_0(n, K) \tag{14}$$

where $\bar{\phi} = M_0/(\mu TLW)$. For given n, ϵ_0 can be made small if a sufficiently large K is chosen. After simplifying (14), we get:

$$\epsilon_0(n, K) \leq \frac{2}{\pi^3 \sqrt{2\pi(K+4)}} \left(\frac{3en}{K+4} \right)^{K+4} \tag{15}$$

So, for $\epsilon_0 \ll 1$, K should be greater than $3en - 4$. For non-ideal observations, when moments are known with relative accuracy δ, a new estimate of ϵ would be:

$$\epsilon < \epsilon_0(n, K) + \delta \pi^{-3} (e^n - 1)^3 \tag{16}$$

The second term does not depend on K, and, for a given K, can be made small only when δ is low. These results are practically independent of the particular window function, if $\tilde{h}$ decreases sufficiently quickly at $\omega \to \infty$, $k_1 \to \infty$ and $k_2 \to \infty$.

Let us make some comments here. The initial stability problem in the estimation of ϕ (or f^{Σ}) from u was related to the need to estimate the spectrum $\tilde{\phi}$ in the whole space (ω, k_1, k_2) from its values given only in the neighbourhood of zero. When we limit the problem and estimate the spectral function only in the specified neighbourhood, the problem becomes corrected, but only the low-frequency component of ϕ can be reconstructed.

Numerical analysis of formulas (150) and (16) shows that, with increasing n, the necessary accuracy δ of moments (and seismograms) grows with n exponentially, and the necessary maximum degree of moments grows linearly. The necessary number of observations for degree K is $(K+1)(K+2)/2$, i.e., it grows as a square of K. Numerical estimates show that even for $n = 4$ (total pixel number is $4^3 = 64$), values $K = 28$ and $\delta = 2 \cdot 10^{-4}$ are necessary, if we wish to know ϕ^* with an accuracy of about 10%. The minimum number of observations in this case is 435. It is clear that the

present theoretical results have little chance of finding practical applications in the near future. They are however interesting, in principle, and could eventually lead to a more practical approach.

Determination of pulse power moments and seismic moment tensor for a deep earthquake

In the rest of this paper we will demonstrate the practical approach to the inversion described in the first two sections. We should take into account that our equations are valid, strictly speaking, only for a homogeneous, unbounded, perfectly elastic medium. We shall assume, however, that the usual technique for interpreting teleseismic body wave records of deep earthquakes is applicable (e.g. Randall, 1972), that is to say, we assume that P, pP, sP and S phases can be separated on the seismogram and that, after deconvolution of the instrument and Q-operator, they can be reduced to the focal sphere. We neglect the effects of the layered Earth structure at receiver and reflection points and consider the wave front flat at the receiver. Note that in this case we only need to account for free surface and for geometrical spreading when finding the seismic moment tensor; this is not necessary for power moment determination.

We used records of body waves from the deep earthquake of February 15, 1971 (depth $H = 574$ km, $m_b = 5.7$, $t_0 = 07\text{h}51\text{m}$, $\phi = 25.20°\,\text{S}$, $\lambda = 178.41°\,\text{E}$, Fiji Islands). Data concerning the stations and phases used are given in Table 1. The records of phases P, pP, sP on vertical channels and of S on horizontal channels of WWSSN LP instruments were optically magnified and digitized; SH records were computed. The digitization interval was 0.1 s, and the data window was 50–70 s. The records were deconvolved for instrument and Q-operator. To do this, the record spectrum was divided by the instrument transfer function and by the medium transfer function $P(f)$. We accepted $|P(f)| = \exp(-\pi f t^*)$. The phase of $P(f)$ was calculated as the Hilbert transform of $\log|P(f)|$. Using Aptekman and Bogdanov (1981) for P-waves, $t_p^* = 0.66$ s was accepted. To calculate t_{SH}^* we accepted $Q_p = 1.6\,Q_s$ and $C_p = 1.8\,C_s$, which gave $t_{SH}^* = 1.9$ s. For pP and sP, t^* values for two legs were summed. For the second leg, t^* was taken as 0.85 s (for surface focus). For the first leg of pP, $t^* = 0.26$ s was computed from $Q(H)$ of Aptekman and Bogdanov (1981) and for sP that value was multiplied by $1.6 \cdot 1.8$. The resulting values were $t_{pP}^* = 1.11$ s and $t_{sP}^* = 1.6$ s.

TABLE 1

The station and phase parameters *

Station code	Δ (°)	Az (°)	j(°)		
			P	pP	sP
RIV	25	244	116	–	37
TAU	31	227	120	–	–
RAB	32.5	305	122	–	–
PMG	33.5	392	122	–	–
GUA	51	316	132	–	26
MUN	54	248	134	51	26
DAV	60.5	295	138	–	–
SPA	65	180	140	–	–
BAG	70	300	143	–	–
MAT	72	327	144	–	–
SHK	73.5	322	145	–	–
ANP	74	308	145	–	–
HKC	78	302	147	–	–
COR	87.5	37	151	–	–
TUC	88.5	53	152	–	–
CHG	89	291	152	–	16
DUG	91	46	152	–	16
COL	93.5	14	–	–	15
ANT	97	120	–	28	–
NNA	98	107	–	28	–
LPA	100	136	–	28	–

* Δ is the epicentral distance, Az is the epicentre to the station azimuth, j is the angle of incidence at the source measured from zenith; j for P and S rays coincide.

To minimize the deconvolution noise generated by the decrease of the composed transfer function at low (because of instrument) and high (because of absorption) frequencies, band pass filtering was applied, with the lower cutoff at 0.01–0.02 Hz, and the upper cutoff depending on the phase type, as follows; 0.7 Hz for P, 0.55 Hz for pP, 0.45 Hz for sP and 0.40 Hz for SH. Then the inverse Fourier transform was applied. Results are plotted in Figs. 1, 2 and 3.

We calculated the unnormalized power moments for body wave pulses for degrees 0, 1 and 2; normalization was carried out for degrees 1 and 2 (see (6)). Pulse beginnings and ends were chosen

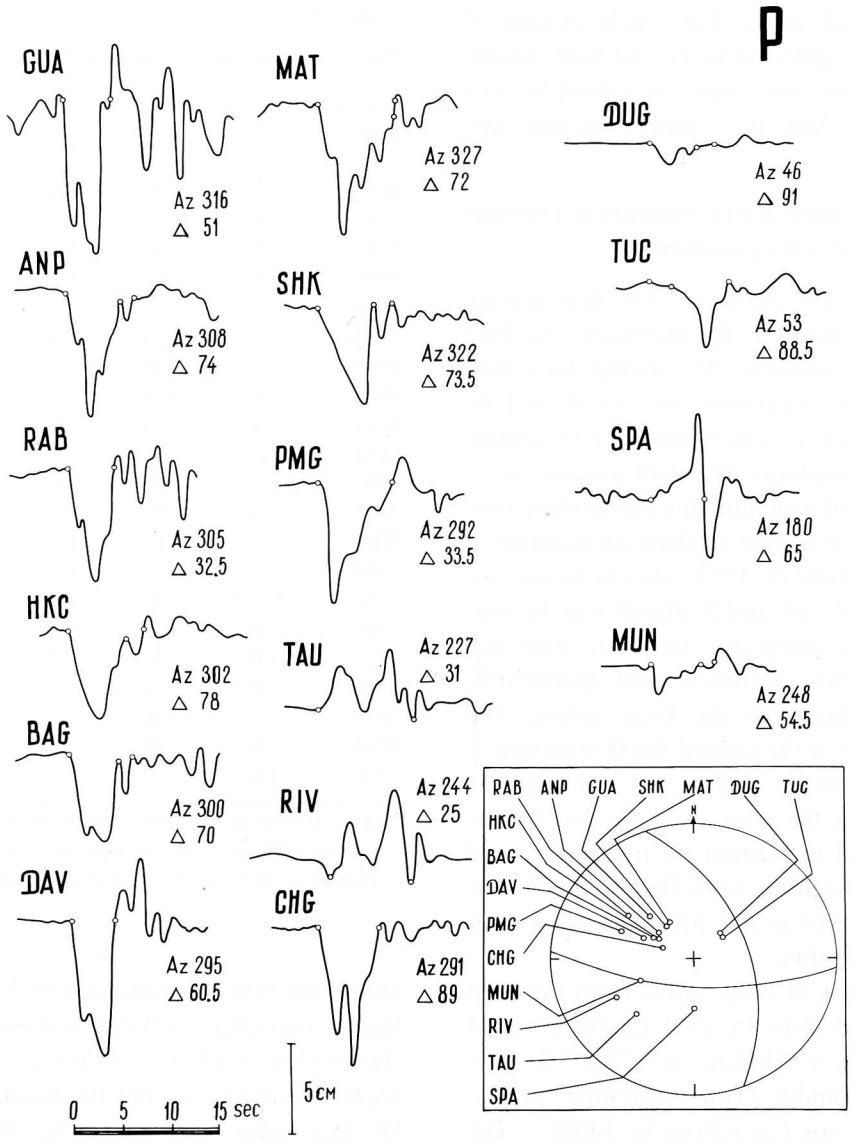

Fig. 1. P-wave pulses after deconvolution of instrument of Q-operators reduced to focal sphere. Geometrical spreading according to (Seismol. Soc. Am., 1968). Circles denote beginning and end points of integration interval. On stereographic projection, incidence points of rays are given and P nodal planes for accepted double couple. Lower hemisphere projection is used here and below (unless otherwise specified).

by eye. In some cases, this choice was not unequivocal, in which case two variants of E_0, e_1 and e_2 were determined.

The E_0 values for the P and SH phases (see Table 2), were used to determine the seismic moment tensor, and e_1 and e_2 were used to determine source power moments. The values of e_1 and particularly e_2 were much more susceptible to noise and to the choice of integration interval than E_0. Thus, several calculated values of e_1 and e_2, which were considered inaccurate, were excluded from further analysis.

To calculate the seismic moment tensor $M_{ij} = M_0 m_{ij}^{(0)}$ from E_0 values, we reduced the data to the focal sphere and then solved the least-squares equations for tensor components. The coordinate system (north, east, up) was accepted. These equations are of the kind:

$$r_i r_j M_{ij} = E_0^{(P)}(\boldsymbol{r}) \cdot 4\pi\rho c_P^3 R_F \qquad \text{(for P)} \quad (17)$$

$$r_i s_j M_{ij} = E_0^{(SH)}(\boldsymbol{r}) \cdot 4\pi\rho c_s^3 R_F \qquad \text{(for SH)} \quad (18)$$

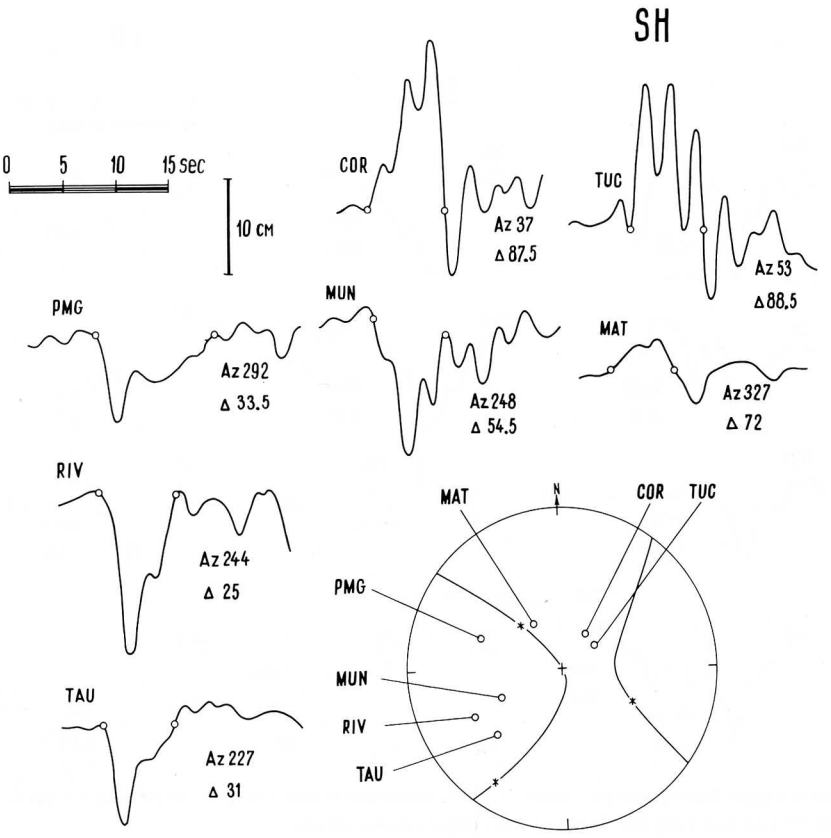

Fig. 2. SH pulses. Stars show eigenvectors of M_{ij} (main variant). Nodal lines for SH for accepted double couple are shown.

where R_F is the radius of focal sphere, and $\boldsymbol{s}$ is defined as $\boldsymbol{s} = \boldsymbol{r} \times \boldsymbol{e}_3 / |\boldsymbol{r} \times \boldsymbol{e}_3|$; $\boldsymbol{e}_3 = (0, 0, 1)$ is directed towards the zenith.

Our main aim was to find out whether M_{ij} corresponds to a double couple source or not. So we tried several variants in our computations. We tried three variants of geometric spreading: computed from tables (Seismol. Soc. Am., 1968) from Aptekman and Bogdanov (1981), where model B1 (from Jordan and Anderson, 1974) was used; and computed (in Ben-Menahem and Singh, 1972) from Jeffreys-Bullen tables for $H = 380$ km. Different data sets included P-waves, P- and SH-waves and SH- and SV-waves. In the case of SV-waves, E_0 was computed from the E_0 for SH and the observed polarization angle. We should note that when only SH data are used, the least-squares system becomes ill-defined, and even when SH and SV data are used, the trace of M_{ij} cannot be determined. To find out if the results were biased by PcP and ScS phases, subsets of data with $\Delta \leqslant 75°$ were used. In another test, we used in dubious cases E_0 values with only "long" or only "short" variants of integration interval. In all, 32 variants of M_{ij} were computed.

To analyze the results, let us introduce the values $\alpha = \frac{1}{3}(M_{11} + M_{22} + M_{33})$ for the isotropic part of M_{ij}, and:

$$\beta = 2\frac{M_{22}^* - M_{33}^*}{M_{11}^* - M_{33}^*} - 1$$

for the "Lode-Nadai coefficient". Asterisks again denote ordered eigenvalues. When $\alpha = 0$, the source is of the pure shear type, and when additionally $\beta = 0$, the source corresponds to a double couple source, or to plane shear rupture. Hypotheses $\alpha = 0$ and $\beta = 0$ were tested using the accuracy measures of M_{ij} components known from the least-squares technique, and accuracy measures of M_{ii}^* determined from the first by the Monte-Carlo type technique. Estimates of the variance and covariance of M_{ii}^* were also computed by repeated least-squares M_{ij}^* determina-

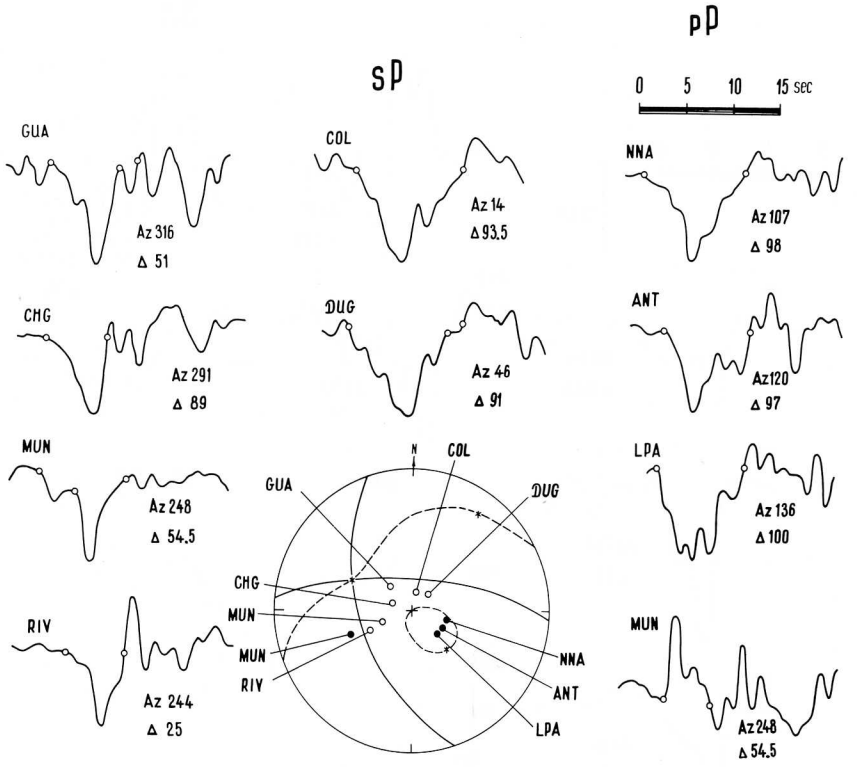

Fig. 3. pP and sP pulses. Upper hemisphere projection is used. Incidence points are dots for pP and circles for sP. Nodal lines for P (continuous lines) and SV (dashed line) are shown, for accepted double couple.

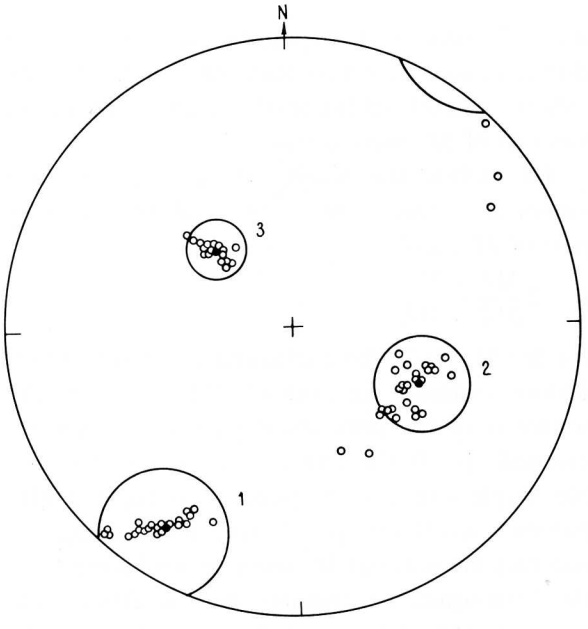

Fig. 4. Eigenvectors of M_{ij} for all variants of computation. Dots—for main variant. Vectors are numbered in order of decreasing eigenvalues. Computed error regions for main variant are also shown.

tion in the coordinate system defined by eigenvectors of M_{ij}. Both techniques gave the same results. M_0 values were estimated as $(M_{11}^* - M_{33}^*)/2$. When $\alpha = 0$ and $\beta = 0$, this estimate is accurate, and is acceptable when deviations from double couple are small. Let us consider now the results of these computations:

(1) *Eigenvector directions* (Fig. 4). Error regions for these directions have dimensions from 10° to 30°, as a rule below 20°, and between variants these directions change only slightly.

(2) *M_0 value*. The main causes of error in estimating M_0 are, first, the variant of geometric spreading (deviations up to 1.7 times) and, second, the wave type (M_0(P) is some 30% greater than M_0(S)). The second deviation could have been produced by an inaccurate t^*_{SH} value. We repeated the deconvolution of SH phases with t^* increased to 2.2 s; the M_0 value stayed practically the same. M_0 errors as a result of factors mentioned are much greater than the formal least-squares errors. We can imply that the real M_0 accuracy is de-

termined by the accuracy of velocity and Q-Earth model, and cannot be revealed when only one fixed Earth model is used in computations. Another implication is that results from the "mixed" data set (P + SH) can be unreliable.

(3) *Value of the isotropic component (α).* All α estimates are less than 10% of M_0; none of them are significant statistically, so the source can be regarded as a pure shear one.

(4) *Coefficient β.* When only P or only S data are used, β estimates are 0.2–0.3, and $\sigma(\beta) =$ 0.25–0.40. With mixed data, the β estimate becomes 0.3–0.4, and $\sigma(\beta)$ decreases to 0.2, as the amount of data is increased. We suppose this phenomenon to be related to non-uniformity produced by the merging of P and S data. Detailed analysis of station geometry, and the structure of equations and residuals justifies this assumption.

TABLE 2

Input data for calculations of seismic moment tensors and source power moments *

Station code	Phase	E_0 (cm s)		e_1 (s)		e_2 (s^2)	
		1	2	1	2	1	2
RIV	P	22.13	–	3.98 **	–	4.06 **	–
TAU	P	11.7	–	5.15 **	–	6.71 **	–
PMG	P	−19.3	–	2.83	–	2.51	–
RAB	P	−16.7	–	2.53	–	1.21	–
GUA	P	−25.1	–	2.23	–	1.19	–
DAV	P	−21.2	–	2.36	–	1.11	–
CHG	P	−20.8	–	2.98	–	1.89	–
BAG	P	−19.6	−17.2	2.96	2.66	1.95	1.25
ANP	P	−19.1	−17.5	2.66	2.42	1.95	1.27
HKC	P	−18.1	−15.6	3.31	2.95	2.68	1.60
MAT	P	−27.9	−20.5	3.63	3.10	3.31	2.25
SHK	P	−19.5	−18.2	3.68	3.39	2.34	1.60
MUN	P	−4.18	−3.86	2.36	1.83	2.47	1.38
SPA	P	7.81	–	3.62	–	1.57	–
TUC	P	−9.20	−7.31	4.76	3.32	2.61	1.11
DUG	P	−3.50	−2.92	2.85	2.20	3.23	1.20
NNA	pP	–	–	5.00	–	3.23	–
LPA	pP	–	–	3.83	–	4.10	–
ANT	pP	–	–	3.94	–	4.44	–
MUN	pP	–	–	1.69	–	1.18	–
RIV	SH	−40.6	–	2.59	–	1.40	–
TAU	SH	−22.2	–	2.16	–	1.94	–
MUN	SH	−48.6	–	3.41	–	2.35	–
PMG	SH	−34.6	–	3.54 **	–	5.94 **	–
MAT	SH	14.7	–	3.28	–	1.97	–
TUC	SH	70.8	–	2.89	–	3.08	–
COR	SH	75.0	–	3.94	–	2.86	–
MUN	sP	–	–	1.72	4.43	0.90	3.64
RIV	sP	–	–	4.32	–	1.35	–
CHG	sP	–	–	4.21	–	1.41	–
GUA	sP	–	–	3.94	4.08	1.74	2.61
COL	sP	–	–	4.80	–	5.51	–
DUG	sP	–	–	4.76	5.87	4.10	6.55

* Values E_0 correspond to the focal sphere of radius $R_F = 1$ km; for pP and sP, they were not computed. In many cases, two variants of integration interval, denoted 1 and 2, were used; variant 1 corresponds to the main variant of source power moment computation.

** Excluded in the main variant.

For unmixed data, the estimated β value does not differ significantly from zero and the simple shear ($\beta = 0$) model can be considered acceptable. The choice of integration interval has been shown to be of minor importance. Residual error does not decrease when data with $\Delta > 75°$ are excluded; so core phases seem not to bias our results.

Taking all this into account, for the final calculations we used inversion with the complete P-wave data set and with Herrin's spreading. The choice of wave type and of the variant of spreading was somewhat arbitrary; however, this is not important for our purposes because the properties $\alpha = 0$, $\beta = 0$ (double couple) and the eigenvector directions were practically independent of the data set. Eigenvalues and eigenvectors for the accepted inversion are given in Table 3 ($\alpha = -0.03 \pm 0.12$, $\beta = 0.31 \pm 0.43$). For the accepted double couple, the axes were taken to coincide with the first and third eigenvectors. The value of M_0 is $1.14 \cdot 10^{26}$ dyn cm. Fault planes can be seen in Fig. 1. This solution was additionally tested using pP data and S polarization angles. It should be noted that in several cases, the signs of P and pP areas (used here) were opposite to the signs at the onset of the same phases. This fact partly explains why our solution differs from previous ones (Balakina et al., 1980; Starovoyt et al., 1983).

Determination of source power moments of degrees 1 and 2 for a deep earthquake

The pulse power moment values e_1 and e_2 of phases P, SH, pP and sP were used to calculate source power moments: the 3-D ones N_α and $N_{\alpha\beta}$ (α, $\beta = 0, 1, 2, 3$), and the 2-D ones $\overline{N}_\alpha$ and $\overline{N}_{\alpha\beta}$ (α, $\beta = 0, 1, 2$). Beforehand, corrections were added to e_1 and e_2 values to compensate for the deviations produced by low-pass (high-cut) filtering. The resulting values are given in Table 2. Then the least-squares technique was applied to eqns. (11) and (12) using 33 phases, with some definite (No. 1 in Table 2) variant of integration interval for each variant. For three phases, the residuals were greater than twice the standard deviation, and so these phases were excluded. The variant of inversion with the remaining 30 phases was considered as the main one. To test the stability of the result, an additional 11 variants of inversion were carried out. In these variants, we (more or less at random) either excluded several phases or used values of pulse power moments obtained with another variant of integration interval.

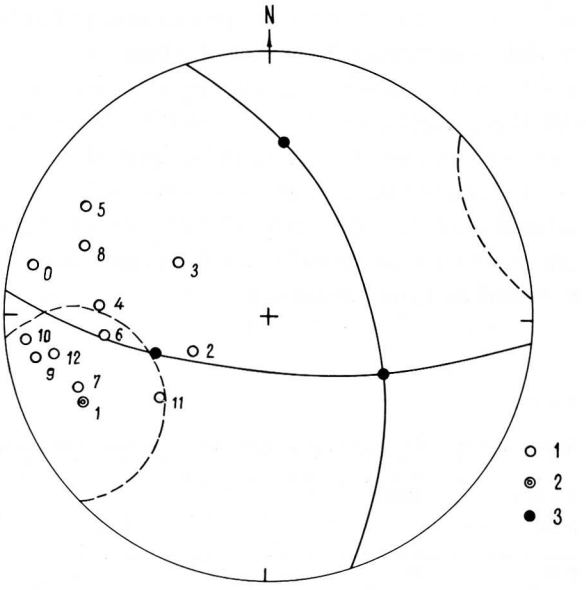

Fig. 5. Directions of $\boldsymbol{q}$ for different variants of 3-D computation. *1* = for all variants except the main one (No. 1); *2* = for the main variant; *3* = eigenvectors of seismic moment tensor. Dashed lines show the error region of direction of $\boldsymbol{q}$ for the main variant.

These calculations showed that the least-squares accuracy estimates for the main variant as a whole describe well the real accuracy of the results. To illustrate the dispersion of these variants, directions of $\boldsymbol{q}$ for the variants are shown in Fig. 5. Dispersion of $\boldsymbol{l}^{(1)}$ is nearly the same as of $\boldsymbol{q}$, and the dispersion of $\boldsymbol{d}$ directions is lower. The results of computation for the main variant are given in Table 4. In Fig. 6, directions are shown for vectors $\boldsymbol{d}_A$, $\boldsymbol{q}_A$ and $\boldsymbol{l}_A^{(1)}$ (from 3-D moments), and for the normals $\boldsymbol{n}_I$ and $\boldsymbol{n}_{II}$ of nodal planes. From these results it can be seen that for the N_{11}^* value and $\boldsymbol{l}^{(1)}$ direction the estimates are stable, while for both the other eigenvalues the estimates differ insignificantly from zero. Moreover, the directions of vectors $\boldsymbol{d}$, $\boldsymbol{q}$ and $\boldsymbol{l}^{(1)}$ are near. In these circumstances, the focal plane cannot be determined from the power moment data only, and the information on M_{ij} must be added. From Fig. 6 we see

TABLE 3

Seismic moment tensor estimates (main variant) *

i	M_{ii}^*	$\sigma(M_{ii}^*)$	Az (°)	j (°)	δ (°)
1	0.99	0.31	34	79	15
2	0.20	0.34	115	129	15
3	−1.29	0.09	137	41	10

* M_{ii}^*, $\sigma(M_{ii}^*)$ are eigenvalues and their standard deviations in units 10^{26} dyn cm; Az, j are azimuth and "angle of incidence" for the corresponding eigenvector; δ is half of the angle of "standard error cone" of the eigenvector.

that all the named vectors are near to one and only to one of two nodal planes (I), so the source plane can be determined: $\boldsymbol{n}$ has $j = 113°$ and $\mathrm{Az} = 4°$ (and $\boldsymbol{b}$ has $j = 48°$ and $\mathrm{Az} = 71°$).

Now we can change the coordinate system (new x_3 along $\boldsymbol{n}$) and apply conditions (5). The results of computations in this case (B) are given in Table 4 and Figs. 6 and 7. They differ only slightly from the 3-D results, and again, the eigenvalue $\bar{N}_{22}^*$ cannot be determined. The estimate of it is negative, but this result is insignificant. Other results

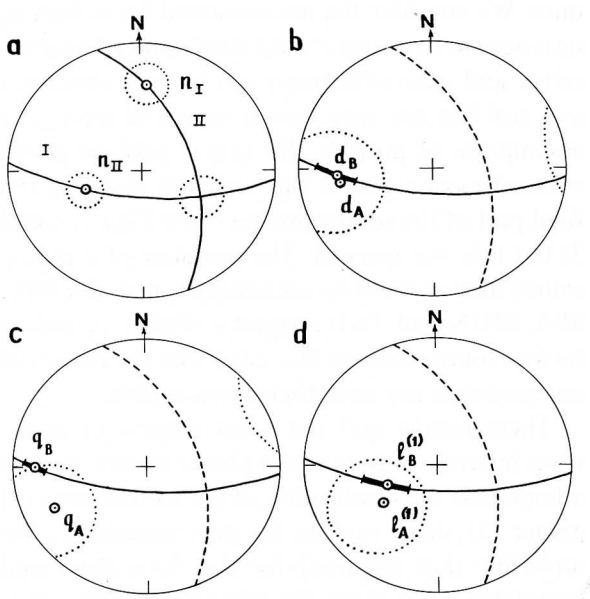

Fig. 6. Comparison of direction estimates in 3-D and 2-D calculations. a. P nodal planes; variants of source plane with normals $\boldsymbol{n}_I$ and $\boldsymbol{n}_{II}$. b, c and d. Vectors $\boldsymbol{d}$, $\boldsymbol{q}$ and $\boldsymbol{l}^{(1)}$. Dotted ovals are error regions for 3-D estimates, solid bars are the same for 2-D estimates.

TABLE 4

Source power moment estimates and derived values

Parameter	Model [a]	
	A	B
N_t (s)	3.61 ± 0.17	3.62 ± 0.16
d		
d (km)	8.8 ± 2.7	8.9 ± 2.3
Az (°)	−98	−95
j (°)	110	109
N_{tt} (s^2)	2.80 ± 0.33	2.70 ± 0.23
q		
q (km s)	7.9 ± 2.2	8.3 ± 1.7
Az (°)	−115	−90
j (°)	105	100
N_{11}^* (km^2)	60 ± 26	57 ± 19
$\boldsymbol{l}^{(1)}$		
Az (°)	54	67
j (°)	54	44
N_{22}^* (km^2)	−2.2 ± 33	−47 ± 33
$\boldsymbol{l}^{(2)}$		
Az (°)	−162	111
j (°)	42	124
N_{33}^* (km^2)	−127 ± 94	–
$\boldsymbol{l}^{(3)}$		
Az (°)	130	–
j (°)	109	–

[a] For B model, Az and j are given in initial coordinate system.

are physically reasonable, and provide information on the space–time source structure.

Interpretation of results

Space characteristics. The "static source" is elongated in $\boldsymbol{l}^{(1)}$ direction, $R_1 = 7.5 \pm 1.3$ km, $L_H = 26 \pm 4.5$ km. As R_2 is not determined, we can suppose that the source area is elongated ($W_H < (0.5–0.3) L_H$). The static source centroid is shifted by $d = |\boldsymbol{d}| = 9 \pm 2.3$ km from the hypocentre in the direction of the long axis of the source.

Rupture direction is defined by the direction of vector $\boldsymbol{q}$. It is near to $\boldsymbol{l}^{(1)}$ again, so the source grew along its long axis.

Degree of symmetry. The static asymmetry parameter is $\chi = 0.68 \pm 0.28$, and the dynamic one

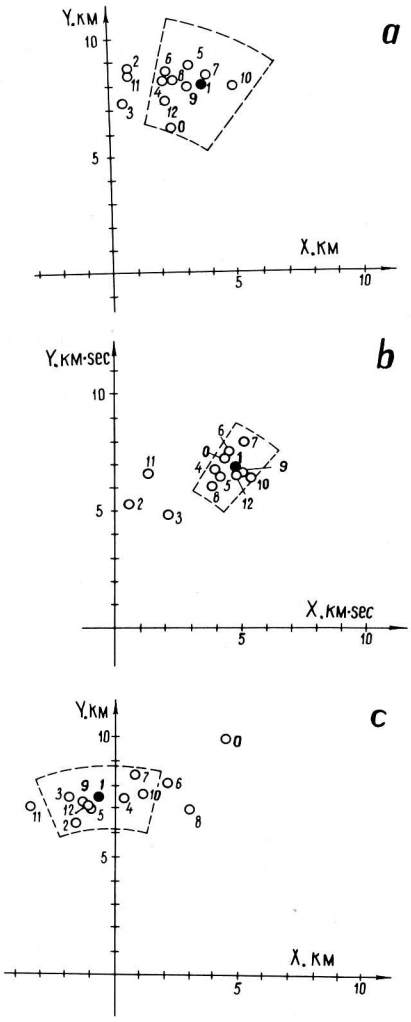

Fig. 7. Estimates of vectors $\boldsymbol{d}$ (a), $\boldsymbol{q}$ (b) and $R_1\boldsymbol{l}^{(1)}$ (c) on the source plane. Y-axis is along $\boldsymbol{b}$. Dashed lines show error regions.

is $\lambda = 0.6 \pm 0.3$. So the rupture is rather asymmetric but not perfectly unilateral.

Rupture velocity. We note again that rupture velocity estimates are necessarily model-dependent. We have $v_1 = 2.6 \pm 0.5$ km/s, $v_2 = 4.0 \pm 0.7$ km/s, and $v_3 = 5.9 \pm 2.4$ km/s. These estimates do not strongly disagree, their weighted average giving $v = 3.4 \pm 0.4$ km/s $= (0.6 \pm 0.1)c_s$.

Source process duration. $R_t = 1.7 \pm 0.1$ s, $T_H = 6.8 \pm 0.3$ s, $2N_t = 7.2 \pm 0.4$ s. Results agree and are relatively the most accurate.

Slip and stress drop. As we do not know W_H, these estimates are very rough. Assuming $W_H = 0.5L_H$, and accepting $\mu = 1.32 \cdot 10^{12}$ dyn cm^2, we obtain $B = M_0/\mu L_H W_H = 24$ cm and $\Delta\sigma = 2.4$ $M_0/(L_H W_H)^{3/2} = 40$ bar.

Discussion

The power moment technique provides a rather useful and model-free description of the earthquake source process. For the earthquake studied here, the estimated set of power moments of degrees 1 and 2 is physically reasonable, and the Haskell-Aki partly bilateral model appears to be suitable. In fact, $\boldsymbol{d}$, $\boldsymbol{q}$ and $\boldsymbol{l}^{(1)}$ vectors (in the 3-D case) lie near to the fault plane, N_t, N_{tt} and $\overline{N}_{11}^*$ are significantly positive, $d < L_H/2$ and $v < c_S$.

The important advantage of the technique described is that it allows a systematic analysis of the accuracy of the results, using the usual least-squares estimates and the Monte-Carlo type estimates for eigenvalues, eigenvectors and other nonlinear functions of N_α and $N_{\alpha\beta}$. An independent way to test the accuracy was to exclude subsets of observations and change the pulse integration interval.

Several assumptions were made to simplify the inversion, and we shall discuss the most crucial ones. We consider the un-accounted for effects of near-source structure ("cold slab") and of near-receiver and near-reflecting-point layered structures as a real but not very serious source of error. The assumption of positive slip rate is perhaps partly violated (some reverse slip seems to occur in the final part of the source process—see Figs. 1, 2 and 3) but this was ignored. The postulate of a planar source may also not be accurate: P pulses for RIV, SPA, MUN and TAU suggest a slightly curved or broken source surface. We think that the results of our inversion are nevertheless reasonable.

These results and the usual success of inversions in terms of parametric planar models give us a hope that the idealization of (1) monotonous (2) planar (3) shear rupture is often acceptable. We underline that the need for the three numbered postulates arises from the inherent general incorrectness of inversion of far-field data. Therefore this, or some other restrictive set of postulates is unavoidable if a practical technique is to be found. Near-field data cannot help in general cases, but

with reasonable postulates their use can greatly improve resolution.

An important disadvantage of the technique described is that it is not generally applicable to surface-focus earthquakes. However, for a special, and not that uncommon, case Silver and Matsuda (1985) have found a way to obtain useful results. Another possible technique (proposed in Pavlov and Gusev, 1980) is the inversion of squared short-period seismograms for power moments of the "non-coherent brightness" function.

Conclusion

An approach is presented for the description and reconstruction of the space–time structure of an earthquake source using power moments in general and those of degrees 1 and 2 in particular. Application of the technique to a real earthquake is described in detail. The approach appears to be efficient for a deep $m_b = 5.7$ earthquake. The theoretical possibility of the reconstruction of a smoothed source function for a planar source is demonstrated.

Acknowledgements

The authors are grateful to Professor S.A. Fedotov for encouragement, to E.M. Guseva who provided the deconvolution code and to Drs. B. Stump and D.J. Doornbos for their critical reviews of the manuscript.

References

Aptekman, J.Y. and Bogdanov, V.I., 1981. Determination of seismic moment tensor from observations. Izv. Akad. Nauk SSSR, Fiz. Zemli, 1981(10): 14–24 (in Russian).

Backus, G., 1977. Interpreting the seismic glut moments of total degree two or less. Geophys. J.R. Astron. Soc., 51: 1–25.

Backus, G. and Mulkahy, M., 1976a. Moment tensors and other phenomenological descriptions of seismic sources. I. Continuous displacement. Geophys. J.R. Astron. Soc., 46: 341–361.

Backus, G. and Mulkahy, M., 1976b. Moment tensors and other phenomenological descriptions of seismic sources. II. Discontinuous displacements. Geophys. J.R. Astron. Soc., 47: 301–329.

Balakina, L.M., Kogan, S.D. and Polikarpova, L.A., 1980. Seismic moments of deep earthquakes from Fiji–Tonga region. Izv. Akad. Nauk SSSR, Fiz. Zemli, 1980(4): 23–38.

Ben-Menahem, A. and Singh, S.I., 1972. Computation of models of elastic dislocation in the Earth. In: Methods in Computational Physics, Vol. 12. Seismology: Body Waves and Sources. 12. Academic Press, New York, pp. 299–375.

Doornbos, D.J., 1982a. Seismic moment tensors and kinematic source parameters. Geophys. J.R. Astron. Soc., 69: 235–251.

Doornbos, D.J., 1982b. Seismic source spectra and moment tensors. Phys. Earth. Planet. Inter., 30: 214–227.

Friedlander, F.G., 1973. On the inverse problem for wave equation. Proc. London Math. Soc., 3(27): 551–576.

Golzman, F.M., 1971. Statistical Models of Interpretation. Nauka, Moscow, 388 pp. (in Russian).

Gusev, A.A. and Pavlov, V.M., 1978. A system of integral characteristics of earthquake source determined from displacements in far field body waves. Dokl. Akad. Nauk SSSR, 239: 285–292 (in Russian).

Gusev, A.A. and Pavlov, V.M., 1982. Method of power moments in the problem of reconstruction of movement in an earthquake source from its radiation. Vulkanol. Seismol., 1982(5): 61–82 (in Russian).

Gusev, A.A. and Pavlov, V.M., 1986a. An application of power moment method to description of source process of a deep earthquake. Dokl. Akad. Nauk SSSR, 287: 586–590 (in Russian).

Gusev, A.A. and Pavlov, V.M., 1986b. A detailed study of a deep earthquake source of Feb. 15, 1971 (Fiji), as an elastic wave radiator. II. Determination of source power moments of degrees 1 and 2. Vulcanol. Seismol., 1986(6): 67–83 (in Russian).

Jordan, T.H. and Anderson, D.L., 1974. Earth structure from free oscillation and travel times. Geophys. J.R. Astron. Soc., 36: 411–459.

Kostrov, B.V., 1975. Mechanics of the Source of Tectonic Earthquakes. Nauka, Moscow, 176 pp. (in Russian).

Pavlov, V.M. and Gusev, A.A., 1980. On the possibility of reconstruction of movement in the deep earthquake source from far field body waves. Dokl. Akad. Nauk SSSR, 255: 824–829 (in Russian).

Pavlov, V.M. and Gusev, A.A., 1986. A detailed study of a deep earthquake of Feb. 15 1971 (Fiji) as an elastic wave radiator. I. Determination of seismic moment tensor. Vulcanol. Seismol., 1986(1): 61–77 (in Russian).

Randall, M.J., 1972. Multipolar analysis of the mechanisms of deep-focus earthquakes. In: Methods in Computational Physics. Vol. 12. Seismology: Body Waves and Sources. Academic Press, New York, N.Y., 267–298.

Seismol. Soc. Am., 1968. Seismological Tables for P. Bull. Seismol. Soc. Am., 58: 1196–1222.

Silver, P.G., 1983. Retrieval of source-extent parameters and the interpretation of corner frequency. Bull. Seismol. Soc. Am., 73: 1499–1511.

Silver, P. and Matsuda, T., 1985. A source extent of the Imperial Valley Earthquake of Oct. 15 1979 and the Victoria

Earthquake of June 9 1980. J. Geophys. Res., 90(B9): 7639–7651.

Starovoyt, O.E., Chepkunas, L.S., Aptekman, J.Y. and Barmin, M.P., 1983. On the determination of earthquake source mechanisms by computer ES-1030. In: Physics of Seismic Waves and Inner Structure of the Earth. Nauka, Moscow, pp. 86–97 (in Russian).